

# THE USE OF EQUALIZING CONVERTERS FOR SERIAL CHARGING OF LONG BATTERY STRINGS

by

D. C. Hopkins, C. R. Mosling, and S. T. Hung  
Department of Electrical Engineering  
Auburn University  
Auburn, Alabama 36849-5201

## ABSTRACT

The use of serial battery cells for primary, secondary and auxiliary power is common in electric vehicles, space power and uninterruptable power supply (UPS) systems. One difficulty with charging serial cells is maintaining equal charge in all cells regardless of the charging conditions and initial condition of the cells. Continual unequal charging and discharging eventually causes certain cells to degrade rapidly and limits the energy capacity and lifetime of the string. To minimize unequal charging, battery manufacturers use extensive measures to match cells. Though the cells are guaranteed to match initially, aging and unpredictable charging and discharging leave long-term matching speculative. Described is a technique that uses dc-dc converters to shunt energy from cells (or groups of cells) while the entire string of cells is being charged. The amount of charging of each cell can be controlled by varying the amount of diverted energy. The technique does not exclude the use of different capacity cells within the string nor exclude the use of different types of energy storage elements.

## INTRODUCTION

Two basic methods of equalizing charge are overcharging and active equalization. Overcharging (or trickle charging) presents a considerable system design penalty. Given a specified charging time, the charging source must be sized to provide a high charging rate for a portion of the specified time and then deliver a reduced or trickle charge rate for the remaining time. A preferred approach follows the same initial charging cycle, but uses any excess charging capacity of the source as it becomes available to selectively charge the weakest cells. This technique of active equalization must cause portions of the charging current to be diverted past certain cells so that not all cells receive the same charging current.

Three techniques can be used to provide active charge equalization. The first uses linear shunt regulators in parallel with each cell, or a group of cells, to route a portion of the charge past the cells as

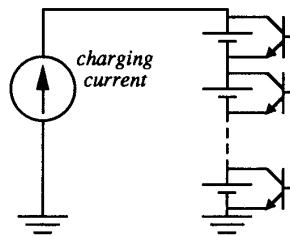


Fig. 1 An adjustable shunt resistance provides a partial bypass for charging current.

shown in Fig. 1. This technique is the least efficient since it extracts the shunt energy as heat. Transistors are shown as an example of controllable devices, however, simple devices, such as zeners, can be used for regulating a fixed cell voltage. The second technique, which implements selective charging, uses dc-to-dc converters to route energy from a common bus to individual cells to provide supplemental energy for equalization. The third technique, which is presented here, actively shunts charge from the cells and recirculates the energy to a common bus.

## System Operation

The circuit model for charging a serial string is shown in Fig. 2. A current source,  $i_s$ , is used to model the energy supply and can be varied to control charging of the entire battery string. A load may be connected to the bus, but for this development, no load is assumed. Charge equalization blocks  $H_1$  through  $H_N$  are step-up converters connected to  $N$  cells (or  $N$  group of cells) with each converter connected to a common bus.

When no converters are operating, the charging current,  $i_c$ , through the string is equal to and controlled by the source,  $i_s$ . With the algorithm used here (for AgZn batteries) the current magnitude in each cell is adjusted to constrain individual cell voltages to less than a maximum cell voltage,  $V_A$ . As the battery string charges, one cell reaches the

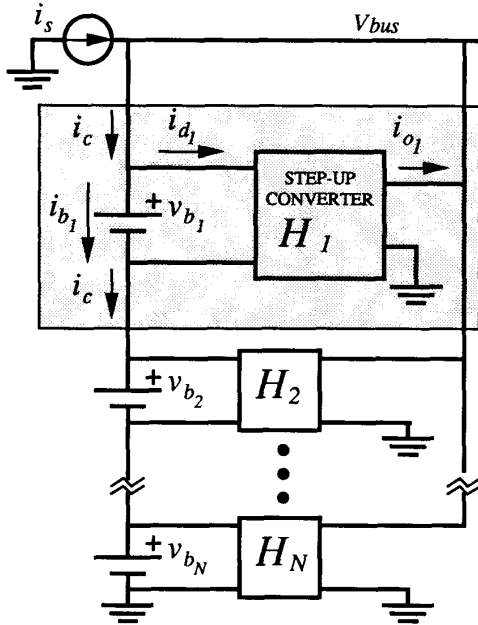


Fig. 2 Circuit model for charge equalization of  $N$  cells or  $N$  groups of cells using equalizing converters.

threshold voltage  $V_A$  and causes its shunt converter to divert current around the cell thus maintaining the cell at  $V_A$ . The diverted current extracts energy, which is placed back into the bus, and appears as an additional charging current to  $i_s$ . This positive feedback, with a gain of less than one, increases the current available for charging the string. As other cells receive higher charging currents some cell voltages will reach the  $V_A$  limit and their converters will activate. The number of converters that can be activated is  $N-1$  if the system is to remain stable (as outlined below). Hence, the charging of  $N-1$  cells is controlled independently of the system while the  $N$ th cell is controlled directly by  $i_s$ . This controlled increase in current (diversion of energy) allows for more greatly depleted cells or cells of larger capacity to be charged at higher rates than available directly from the source.

**Open-Cell Operation.** When using certain batteries, such as  $AgZn$ , there is a risk a cell or group of cells may open circuit upon failure. This would leave the power system defunct. This would leave the power system defunct. However, in this situation the equalization converters, if sized properly, could continue charging and discharging the remaining operational cells. Refer to Fig. 2. If a cell fails, the converter across it will automatically regulate the voltage across the failed cell during charging and allow current to flow in the whole battery string. For energy discharge, the converters across the functional cells can be used in the traditional fashion with their outputs in parallel while the open-cell

voltage is still maintained. This could facilitate the strategy for a redundant power system if required.

### Charge Equalization

Refer to the shaded area of Fig. 2 for the definition of symbols. The battery charging current,  $i_{b1}$ , can be determined from  $i_c$  such that

$$i_c = i_s + i_{o1} + i_{o2} + \dots + i_{on} \quad (1)$$

or can be expanded as

$$i_c = i_s + i_{d1} H_1 + \dots + i_{dn} H_n \quad (2)$$

Then  $i_{b1}$  can be defined as

$$i_{b1} = i_s + i_{d1} (H_1 - 1) + i_{d2} H_2 + \dots + i_{dn} H_n \quad (3)$$

where  $n$  is the number of converters operating and  $H$  is the current gain of the converter. When converter  $H_1$  is off,  $i_{d1} = 0$ , the charging current  $i_{b1}$  is dependent on  $i_s$  and the output current from other operating converters (i.e.  $i_{b1} = i_c$ ). When  $H_1$  is on, the charging current  $i_c$  is decreased by the value of  $i_{d1}$  (i.e.  $i_{b1} = i_c - i_{d1}$ ). The charging current available for the second cell group remains unchanged at  $i_c$ .

As the maximum charging rate of one cell is reached the corresponding converter begins diverting charge, which increases  $i_c$ . As other cells reach

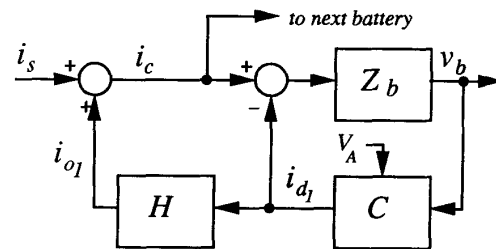


Fig. 3 Power flow diagram where  $H$  is the current gain of the converter,  $Z_b$  is the battery characteristic and  $C$  is the control algorithm for charging.

their maximum charging rate, their corresponding converters start diverting charge until at least one cell has not exceeded its maximum. In this last cell the charging current,  $i_{bn}$  equals  $i_c$  and is controlled directly by the system to regulate the voltage of this cell.

A power flow diagram is shown in Fig. 3 for a single cell and converter, where  $H$  is the current gain of the converter ( $=1/N$ ),  $Z_b$  is the battery characteristic and  $C$  is the control algorithm for charging. Whether a converter is on and to what extent it diverts current depends on the amount  $v_b$  is greater

than  $V_A$ . A further refinement can be made to the diagram which decouples power flow and control. If the characteristics of the converter and cells are considered equivalent, then when  $n$  converters are operating with  $v_{bn} > V_A$ , the resulting power flow diagram for the system simplifies to Fig. 4. As can be seen, the power flow is in a positive feedback path. As more converters begin diverting current into the bus the battery charging current  $i_c$  increases (with  $i_s$  constant).

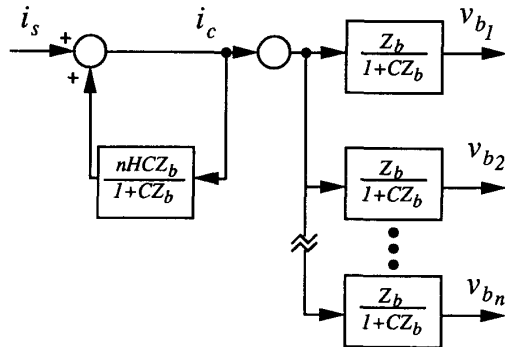


Fig. 4 Simplified power flow diagram with  $n$  of the  $N$  converters operating.

An outer loop, not shown, can be closed around the output voltage  $v_b$  to implement a charging algorithm, such as to regulate  $i_s$  and keep  $i_c$  constant. If it is desired to keep  $i_s$  constant, a larger current is available for charging larger capacity batteries at a greater rate within the serial string. A polling routine or an OR function would determine the lowest  $v_b$  to use for outer loop regulation. Since there must be at least one converter not operating, then at least one  $v_b < V_A$ . The governing system equation is

$$i_c / i_s = (1 + CZ_b) / (1 + CZ_b - nHCZ_b) \quad (4)$$

If the low frequency gain of  $CZ_b \gg 1$ , in steady state as  $t \rightarrow \infty$ , then

$$i_c / i_s \rightarrow 1 / (1 - nH) = N / (N - n) \quad (5)$$

where  $H = 1/N$  for an ideal converter and  $N$  is the total number of converters (or cells). This indicates that stability is achieved when  $n < N$  or, simply, that  $N - 1$  converters is the maximum number that may be on. Implicit in all this is that  $n$  can also represent a percentage of the power that a converter is processing and need not be an integer number.

### SIMULATION OF OPERATION

The operation of the charging system was simulated using EASY5™ [1]. The system model used for the simulation is shown in Fig. 5 with the

expanded details of the battery/converter model of Fig. 3. The details and derivation of each block are given below.

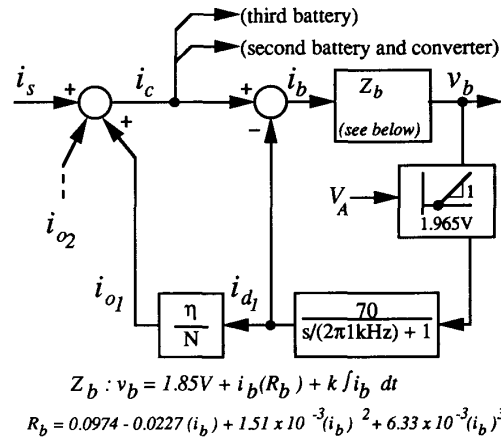


Fig. 5 Simulated model of the system shown in Fig. 4 and applied to the system in Fig. 2 for  $N=3$ .

Control block  $C$  of Fig. 4 represents the controlled input voltage-to-current characteristic (or conductance) of the dc-to-dc converter as it operates above a certain input threshold voltage,  $V_A$ . The block is separated, in Fig. 5, into conductance and dead band blocks. For proof of feasibility, the system was physically realized using a flyback converter, as described later, and given a conductance characteristic with a pole at approximately 1kHz and a 3dB gain of approximately 50. An input filter was also used, but not included in the model.

The system block  $Z_b$ , which represents the battery cell characteristic, is modeled as an open-circuit-voltage source, a current-to-voltage integrator, and a nonlinear resistor which was derived empirically for aged AgZn cells. The characteristic of the resistor changes depending on state of charge and cell condition and cannot be generalized. However, the value used for this development is sufficient to show feasibility of the system. Any change in the characteristic would also be indicative of changes that occur due to aging and variations between different batteries and battery types. For this development the resistance is mathematically approximated by a third order polynomial fitted to the data, as shown in Fig. 6,

$$R_b = 0.0974 - 0.0227 (i_b) + 1.51 \times 10^{-3} (i_b)^2 + 6.33 \times 10^{-3} (i_b)^3 \quad (6)$$

The power flow through the dc-to-dc converter is modelled by the  $H$  block. The converter has a fixed

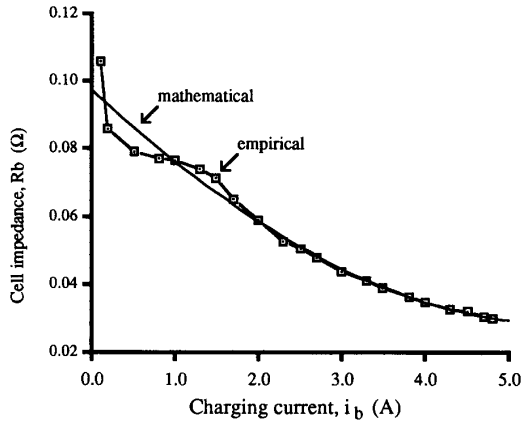


Fig. 6 Battery resistance model for aged AgZn cells.

output-to-input voltage ratio set by the taps on the battery voltage string. If all voltage taps are set for the same value, as is assumed here, then, for the taping of  $N$  cells (or  $N$  groups of cells), the ratio of output-to-input voltage is  $N$ . For a near constant voltage ratio the current is proportional to power. For a converter with an efficiency  $\eta$ , the transfer function for  $H$  is

$$i_{o1} / i_{d1} = \eta / N \quad (7)$$

The governing system equation (5) is then

$$i_c / i_s = N / (N - n \eta) \quad (8)$$

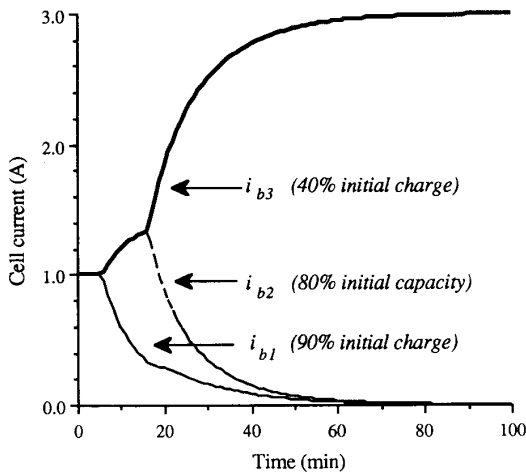


Fig. 7a Simulated charging currents (refer to Fig. 2) when the source is held constant at 1A.

For the simulation an efficiency of 100% was assumed.

The overall configuration of the battery charging system which was simulated is similar to that shown in Fig. 2 for  $N = 3$  and is shown in detail in Fig. 5. The cells from top to bottom (Fig. 2) were set with initial charge capacities of 90%, 80% and 40%, respectively. The bottom converter, connected to the cell with 40% capacity, was assumed not to be activated. Therefore, Fig. 5 does not include feedback loops for the third (or bottom) cell.

The simulation calculated the voltages and currents of the three cells as they charged from a constant source of 1A for 100 minutes. The results are shown in Figs. 7a and 7b. In Fig. 7a the currents through each of the cells is shown. When the terminal voltage of the top cell,  $v_{b1}$ , reaches the threshold voltage,  $V_A$ , as shown in Fig. 7b, the top converter diverts current, decreases  $i_{b1}$ , and increases the current through the other two cells. When the voltage of the middle cell (80% initial capacity) reaches threshold the middle converter diverts and reduces the cell current,  $i_{b2}$ , and further increases the third cell current. The third cell increases each time a converter is activated and, in the limit as  $i_{b1}$  and  $i_{b2}$  approach zero,  $i_{b3} (= i_c) = N i_s = 3A$  as predicted by (5).

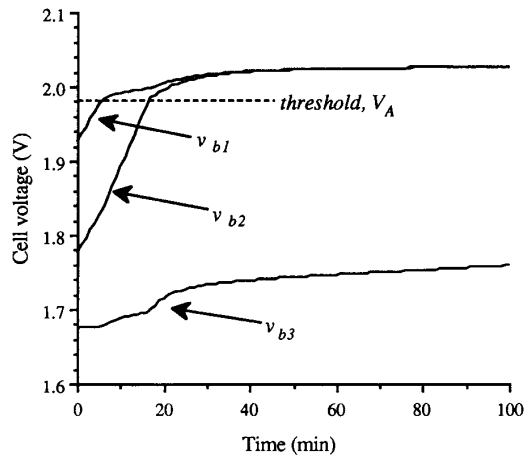


Fig. 7b Simulated cell voltages.

## IMPLEMENTATION

The work described here was initially intended for a solar powered electric vehicle. The electrical system is shown in Fig. 8. The system was designed to have a solar array with peak-power tracking circuits deliver 132V maximum at up to 950W with the bus voltage fixed by the battery terminal voltage. The battery charging current was drawn from the common bus and regulated by controlling the ratio of power produced by the array to that used by the motor load. The 5hp motor operated independently within a given power range and did not provide regeneration

for battery charging. The battery bank was composed of 66 AgZn (silver zinc) cells divided into four serial groups of 16 or 17 cells each. For developing the charge equalization strategy as described in this paper, a bank of thirty AgZn cells are used and grouped into three groups of ten cells each. Since, at

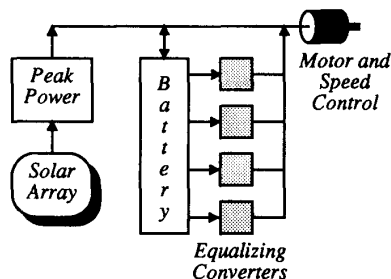


Fig. 8 Solar powered vehicle system.

most, only N-1 converters can be on to maintain a stable system, only two of the three groups of cells have associated converters.

Though AgZn batteries are used as an example, any type of battery or storage system can utilize equalization. Only the algorithm for determining charge capacity and charging profile need be changed. Also, the rating of individual battery groups (i.e. individual series strings) need not be the same. For example, 40 A-hr, 70 A-hr and 100 A-hr rated cells can be charged collectively within one serial string. A further consideration is that the equalization strategy can be applied to any charge storage element.

**Silver Zinc Cell Characteristics.** The battery characteristics are necessary to determine the system and control requirements for implementation of the equalization scheme. The cells used for this development are Whittaker-Yardney Model HR40DC-13 silver zinc (AgZn) cells which have a 40 A-hr capacity. Since the AgZn cells are sensitive to abuse, care was taken not to overcharge or over-discharge the cells. The manufacturer recommends a nominal charge current of 3A to 5A with voltage monitoring so that any one cell voltage is not allowed to exceed 2.05V[2]. The charging efficiency of the cells is higher when they are at a lower state of charge, however, for the concerns of this paper and to make measurements easier, cells with near 100% charge were used for testing.

#### System Realization

The basic system was constructed, as in Fig. 9, with three groups of cells (N=3). The top and middle groups were nearly fully charged while the bottom group was purposely left with a low state of charge. Since at most, N-1 converters can be on, only the two

nearly charged groups needed converters. The bottom group was too low in charge to risk overcharging.

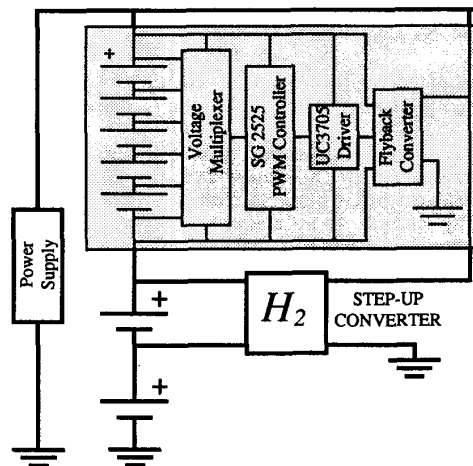


Fig. 9 Circuit implementation of equalization scheme. Shown in the shaded area is a bank of AgZn batteries arranged into five groups with two cells per group for monitoring.

A block diagram of a single converter is shown in the shaded area of Figure 9. The five batteries in the shaded area each represent a pair of AgZn cells with the voltages being monitored across each pair. The control has two main parts, the analog multiplexer and the PWM controller. The analog multiplexer selects the highest voltage of a cell pair and passes it to the SG2525 PWM controller. The error amp of the SG2525 is used as a straight deadband gain circuit with threshold  $V_A$  set at 1.98V per cell. In conventional converter designs, negative feedback occurs at the error amp of the PWM chip. Since this is a shunt type regulator, the negative feedback occurs within the power circuit. The negative feedback, i.e.  $i_{d1}$ , can be seen in the system model of Figure 3. The flyback converter design was used although any step-up topology would suffice.

**Converter Power Rating.** The input power of the converter must match the power level needed to charge the last cell group, i.e. the group with the greatest amount of charge to be replenished. During maximum equalization ( $n = N - 1$ ) each converter must process the maximum charging current,  $I_{c,max}$ . The power rating (output power) of the converter should then exceed

$$P_c = \eta v_{b,max} I_{c,max} \quad (9)$$

where  $v_{b,max}$  is the maximum terminal voltage of the cell group. However, the maximum power available

for charging is limited by the source and can be equated to a maximum available current,  $I_{s,max}$ . A bound on the power rating can then be found from (8). A maximum rating is then

$$P_c = \eta N U_{b,max} I_{s,max} / (N(1-\eta) + \eta) \quad (10)$$

Note that as  $\eta$  approaches 100%, the required converter power approaches the source power.

For system implementation, the approach was taken to maximize the power from the source with  $I_{s,max}$  set at a constant 1.5A from a source voltage of 60V. The converter efficiencies were measured at 75% so the required output power rating was 45W.

### Experimental Results

The system was connected as described above and shown in Fig. 9. The supply current was maintained constant at 1.5A while the voltages and currents of the cells and converters were monitored during the charging. A plot of the currents  $i_{b1}$ ,  $i_{b2}$ , and  $i_{b3}$  through the upper, middle and bottom cell groups, respectively, is shown in Fig. 10. The values of current are normalized by 1.5A source current value. It can be seen that as the upper two groups

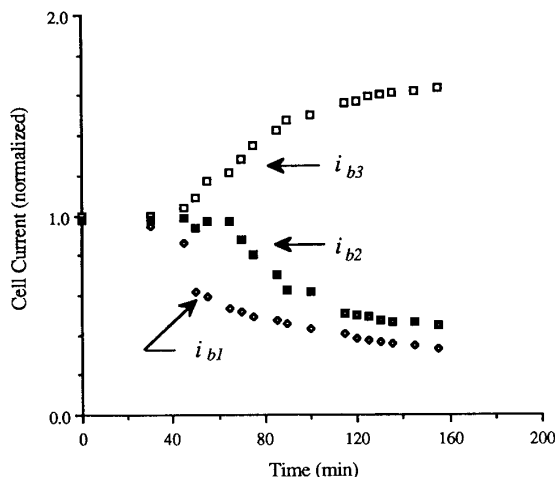


Fig. 10 Empirical results for equalized charging of a string of AgZn cells.

reach maximum capacity their converters begin current diversion and decrease  $i_{b1}$  and  $i_{b2}$ ;  $i_{b3}$  then increases. The overall trend is similar to and verifies the simulation results of Figure 7a. The value of  $i_{b3}$  ( $i_c = i_{b3}$ ) is closely predicted by (2). The branching points of the currents are not as distinct as simulated because the initial state of charge within the cells could not be accurately determined.

### SUMMARY

One difficulty with charging serial cells is maintaining equal charge in all cells regardless of the charging conditions and initial cell conditions. Continual unequal charging and discharging eventually causes certain cells to degrade rapidly and limits the energy capacity and lifetime of the string. Two basic methods of equalizing charge are overcharging and active equalization.

A technique of active equalization allows a portion of the charging current to be diverted past certain cells so that not all cells receive the same charging current. A current source,  $i_s$ , is used to model the energy supply and is varied to control charging of the entire battery string. The remaining system uses dc-dc converters to shunt "cells" (or groups of cells). When no converters are operating, the charging current,  $i_c$ , through the string is equal to and controlled by the source,  $i_s$ . As the battery string charges, one cell reaches a threshold voltage,  $V_A$ , and causes its shunt converter to divert current around the cell thus maintaining the cell at  $V_A$ . The diverted current extracts energy, which is placed back into the charging bus, and appears as an additional charging current to  $i_s$ . This positive feedback, with a gain of less than one, increases the current available for charging the string. This controlled increase in current allows for more greatly depleted cells or cells of larger capacity to be charged at higher rates than available directly from the source. The number of converters that can be activated is  $N-1$  if the system is to remain stable.

If a cell fails, the converter across it will automatically regulate the voltage across the failed cell during charging and allow current to flow in the whole battery string. For energy discharge, the converters across the functional cells can be used in the traditional fashion with their outputs in parallel while the open-cell voltage is still maintained.

### ACKNOWLEDGEMENTS

This project was supported in part by the SOL-OF-AUBURN Solar Powered Race Car Project which provided partial funding and an appropriate test situation. The authors would also like to acknowledge the assistance received from NASA-Marshall Space Flight Center - Electrical Power Branch.

### REFERENCES

1. Boeing Computer Service, "EASY5 Dynamic Analysis System," 1989.
2. T. R. Crompton, *Small Batteries*, John Wiley & Sons, Inc., New York, Vol. 1: Secondary Cells, pp. 160 - 164, 1982.